利用 *W* 波相逆推震源參數與單位海嘯建立琉球海域海嘯預警系統(II)

W Phase Inversions and Seismic Tsunami Warning System in Taiwan for Ryukyu Trench Earthquakes

陳伯飛
中央大學地球科學系

摘要

位於台灣東北的琉球海溝東北西南延伸超過一千公里，具有災害性海嘯地震發生的潛在危機，對台灣構成威脅。本計劃為建立琉球地區地震的海嘯預警系統，方法上沿襲前一建立南中國海海嘯預警系統的計劃，結合單位海嘯與 *W* 波相的逆推。前者將可能震源區(琉球隱沒帶)劃分成單位海嘯源的組合，並事先計算各單位海嘯源的傳播，將虛擬潮位站記錄到的單位海嘯波建立資料庫，此資料庫已可迅速預測海嘯波到時。*W* 波相是大地震所產生非常長週期的地震波，並以高於 *S* 波的群速前進，此快速的長週期波相適合用來迅速逆推得到大地震的震源參數，依據此震源參數計算海底地形的起伏，此起伏作為單位海嘯的權重，經由單位海嘯波的線性組合，便可預測海嘯波的波高。本計劃除資料庫的建立外，也測試過去琉球海溝地區較大地震用區域性地震網所觀測的 *W* 波相逆推震源參數的可行性，結果顯示區域性地震網 *W* 波相逆推琉球地區大地震可得到穩定解。

Abstract

The Ryukyu trench offshore northeast Taiwan, with its NE-SW stretch more than 1000 km, is a potential zone of significant tsunamigenic earthquake to occur, which will cause widespread tsunami hazards in Taiwan. In this study, we propose to establish a seismic tsunami warning system in Taiwan for earthquakes in the Ryukyu trench by combining *W* phase inversion and unit tsunami method. *W* phase is suitable for a rapid determination on the tsunami generation aspects of a large earthquake because it is a long period (100s ~ 1000s) phase with relative fast group velocities (4.5~9 km/s). The unit tsunami method, on the other hand, is able to quickly predict the tsunami waves of a given source by linear combinations of pre-calculated unit-source tsunamis, as pull from the database. In this study, we first test the applicability of *W* phase for past earthquakes in the Ryukyu trench region, using regional seismic array (Broadband Array in Taiwan for Seismology and F-net).

Secondly, we divide the source region of the Ryukyu Trench into squares (1.0° in dimension) of unit source whose tsunami wavefields at current tidal stations in Taiwan are calculated and store in database. Finally, given earthquake source parameters determined from *W* phase inversion, we are able to calculate the weighting of each unit source and predict the amplitudes and arrival times of approaching tsunamis to tidal stations in Taiwan. The tsunami warning system in Taiwan for Manila trench earthquakes is thus established.

1. Introduction

Historically, the tsunami hazards in Taiwan occurred in the North and SW coasts (Soloviev and Go 1974). Those at SW Taiwan are believed to be triggered by earthquakes in the Manila subduction zone and amplified by the steep slope of the South China Sea (SCS) shelf and those in the north are most likely associated with tsunamigenic earthquakes in the Ryukyu subduction zone. In previous project, we have established a tsunami warning system for South China Sea using unit tsunami methods and *W* phase inversion. The purpose of this project is applying the same methodologies to build a tsunami warning system for earthquakes in the Ryukyu subduction zone. Firstly, we introduced methods of unit tsunami and *W* phase inversion. Secondly, we divided the potential source region of the Ryukyu subduction zone into group of unit sources and calculate the propagation of each unit source as unit tsunamis stored in database. Thirdly, we sorted out past large earthquakes in the Ryukyu subduction zone and collected data from Broadband Array in Taiwan for Seismology (BATS; Kao et al., 1998) and F-NET to assess the results of *W* phase inversion. Finally, we conclude this study.

2. Methods and Results

2.1. Building Database of Unit Tsunamis

The potential source region of the Ryukyu subduction zone was divided into 107 square pixels, each with $1.0^\circ \times 1.0^\circ$ in size and an initial vertical seafloor displacement of 1 m was assigned to each pixel to constitute the group of unit sources (Figure 1). We employed Cornell Multigrid Coupled Tsunami Model (COMCOT) to simulate the propagations of each unit source. COMCOT is a finite difference scheme and in our case, we solved for linear shallow water wave equations in spherical coordinates with 1 minute (~1.8 km) and 1 sec in space and time, respectively. The boundary conditions are total reflection for ocean-land interfaces and radiation for map boundaries. We set up 32 virtual stations representing existing tidal stations of Central Weather Bureau (Figure 2). The wave field of one station from one unit source is referred to the unit tsunami corresponding to the station-unit source pair. For each unit source, we simulated for four-hour propagations (Figure 3) with the resulting wave fields as a function of time at the 32 stations stored in database (Figure 4). In the end, a total of 107×32 unit tsunamis were stored in database for synthetics of tsunami waves in real events. The stored unit tsunamis are readily available for arrival time predictions even without the occurrence of real events. We applied Short Time Average over Long Time average (STA/LTA; Allen 1982), a conventional

scheme for picking seismic P and S phases, to automatically pick the arrival times of unit tsunamis (Figure 5) with results shown as arrival time map (Figure 6) and stored in database for arrival time predictions.

2.2 *W* Phase Inversion

We refer readers to Kanamori and Rivera (2008) regarding theory, modeling, and source inversion of *W* phase. We recapitulate here that *W* phase can be interpreted as superposition of the fundamental mode, first, second and third overtones of spheroidal modes at long period and can be synthesized by normal-node summation. The Green's functions of six moment tensor elements are pre-computed for a distance range of $0° \leqq \Delta \leqq 90°$ with an interval of 0.1° and for a depth range of 0-760 km. The synthetic waveforms of an earthquake are derived by convolving the Green's function with its moment rate function, which is a triangular function defined by two parameters, half duration, t_h, and the centroid delay, t_d (Figure 7). The broadband seismic data are deconvolved to displacement with instrument response removed and a band-pass filtered. A time period of 15Δs (Δ epicentral distance in degree) from the beginning of *P* wave is windowed to extract W phase. A time domain recursive method is used not only for real time operation but also for using available data to the point where it gets clipped at the large amplitude *S* or surface waves. The same procedures are applied on synthetic waveform and, together with data, a linear inversion is performed on concatenated time series using a given hypocenter location and origin time.

We sorted out earthquakes between Jan. 2000 and July 2011 with moment greater than 10^{25} dyn-cm and bounded by (10°N, 26°N) and (115°E, 135°E) from the GCMT catalogue (Dziewonski et al., 1981; Ekström et al., 2005). Figure 8 shows the distribution of earthquakes. A visual regional array, including the bulk of current BATS and selected stations from F-NET is set up to conduct *W* phase inversion (Figure 8). The LH channel data (1 smaple-per-second) of earthquakes from the array are collected through Web site for source inversion of *W* phase and the results are compared to GCMT solutions of the same event. Some stations are eliminated with their data continually exhibit low quality (e.g., LYUB). We tested for six scenarios divided into two groups: using vertical component only and using all three ZNE components. In each group, three sets are tried with different level of knowledge on earthquake parameters: (1) using the GCMT centroid parameters (not practical in real case), (2) using the hypocenter parameters (lon., lat., depth, origin time) reported by the PDE (Preliminary Determination of Epicenters) catalogue, and a centroid time, t_d, determined by grid search; the source half duration, t_h, is set equal to t_d, (3) the same as (2) except the centroid location (lon., lat.) determined by a 2-dimensional grid

search (depth fixed at PDE's). We present the results with gCMT location, t_d location, and (t_d+xy) location, respectively. The cutting distance – within which data are removed – is determined to be 1.0°. The inversion is iterated three times with a higher threshold is assigned on each to keep data for inversion. An example of fitting between synthetic and observed waveforms of vertical component for the 20090805 event is shown (Figure 9). The frequency band used to filter seismic waveforms basically follows Table 1 of Hayes et al. (2009).

We present the comparisons of M_w (GCMT) and M_w (W phase) for each of six scenarios in Figure 10, with the mean values of absolute magnitude differences and their standard deviation shown. We note that the results ZNE components are significantly better than their counterparts of Z component only. Column-wise, solutions of gCMT location exhibit least mean values of magnitude differences regardless vertical components only (left column) or ZNE three components (right column). However, the GCMT parameters are not available in real time application. Among the remaining four scenarios, the one with least value of magnitude difference is results of t_d location with three components (right column, middle). The larger events (M_w > 6.6) also tend to exhibit more consistent results with those of GCMT solutions. This implies that using PDE hypocenter and grid searching for t_d on ZNE three component data can serve as routine operational procedures for *W* phase inversion of SCS earthquakes.

3. Conclusions

In this study, following previously proposed combining *W* phase inversion and unit tsunami methods, we build a tsunami warning system in Taiwan for earthquakes in the Ryukyu subduction zone. The *W* phase inversion allows us to rapidly determine moment tensors of large earthquakes for the calculations of vertical seafloor displacements (Okada, 1985). The applicability of *W* phase inversion for Ryukyu subduction zone earthquakes using BATS stations and some of F-net stations has been tested and the best scenario determined to be t_d location with three components. We have built a database of unit tsunamis for the source region of the Ryuku subduction zone and the prediction of arrival times is readily available once the epicenter of tsunamigenic earthquake is known.

4. References

1. Allen, R., 1982. Automatic phase pickers: their present use and future prospects. Bull. Seismol. Soc. Am. 72(6), 225-242.
2. Dziewonski, A., M., Chou, T.-A., Woodhouse, J.H., 1981. Determination of

earthquake source parameters from waveform data for studies of global and regional seismicity. J. geophys. Res., 86, 2825-2852.

3. Ekström, G., Dziewonski, A.M., Maternovskaya, N.N., Nettles, M., 2005. Global seismicity of 2003: centroid-moment-tensor solutions for 1087 earthquakes, Phys. Earth planet. Inter., 148(1-2), 327-351. Global CMT catalog; GCMT. http://www.globalcmt.org.
4. Hayes, G.P., Rivera, L., Kanamori, H., 2009. Source inversion of the W-phase: real-time implementation and extension to low magnitudes. Seismological Research Letters, 80(5), 817-822 doi: 10.1785/gssrl.80.5.817
5. Kao, H., Jian, P.R., Ma, K.F., Huang, B.S., Liu, C.C., 1998. Moment-tensor inversion for offshore earthquakes east of Taiwan and their implications to regional collision. Geophys. Res. Lett. 25, 3618-3622.
6. Kanamori, H., Rivera, L., 2008. Source inversion of W phase: speeding up seismic tsunami warning. Geophys. J. Int., 175, 222-238 doi: 10.1111/j.1365-246X.2008.03887.x
7. Kanamori, H., Rivera, L., 2009. Application of the W phase source inversion method to regional tsunami warning. In press.
8. Okada, M., 1985. Surface deformation due to shear and tensile faults in a half-space. Bull. Seismol. Soc. Am. 75(4), 1135-1154.
9. Soloviev, S. L. and Ch. N. Go, 1974: A catalogue of tsunamis on the western shore of the Pacific Ocean (173-1968). Nauka Publishing House, Moscow, USSR, 310 pp. Can. Transl. Fish. Aquat. Sci. 5077, 1984.

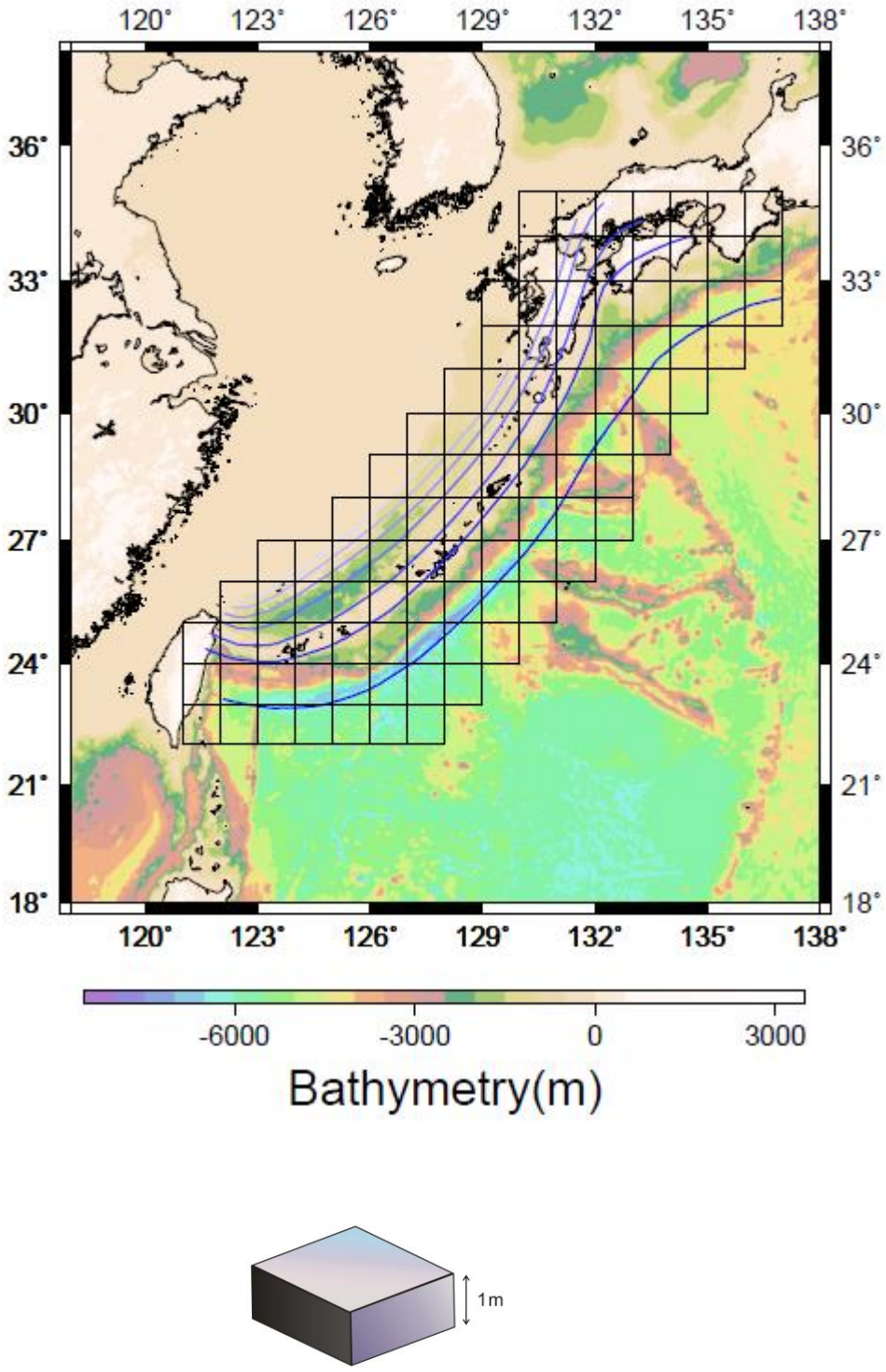

Figure 1: (Top) Division of the Ryukyu subduction zone into 107 pixels of unit sources. (Bottom) The one-meter initial vertical displacement assigned as unit source.

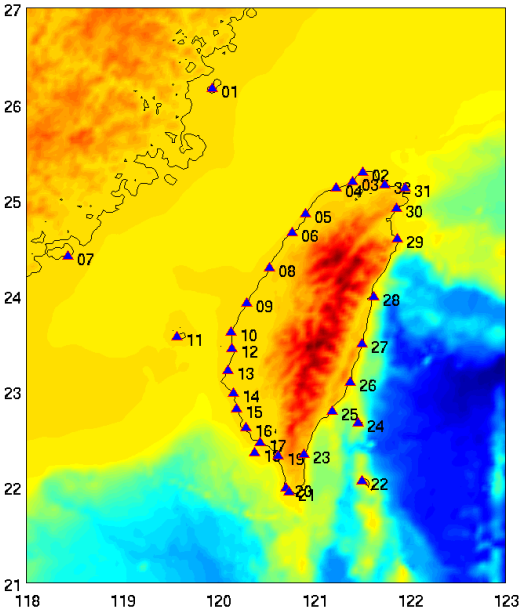

Figure 2: Numbering of CWB tidal stations for recoding unit tsunamis.

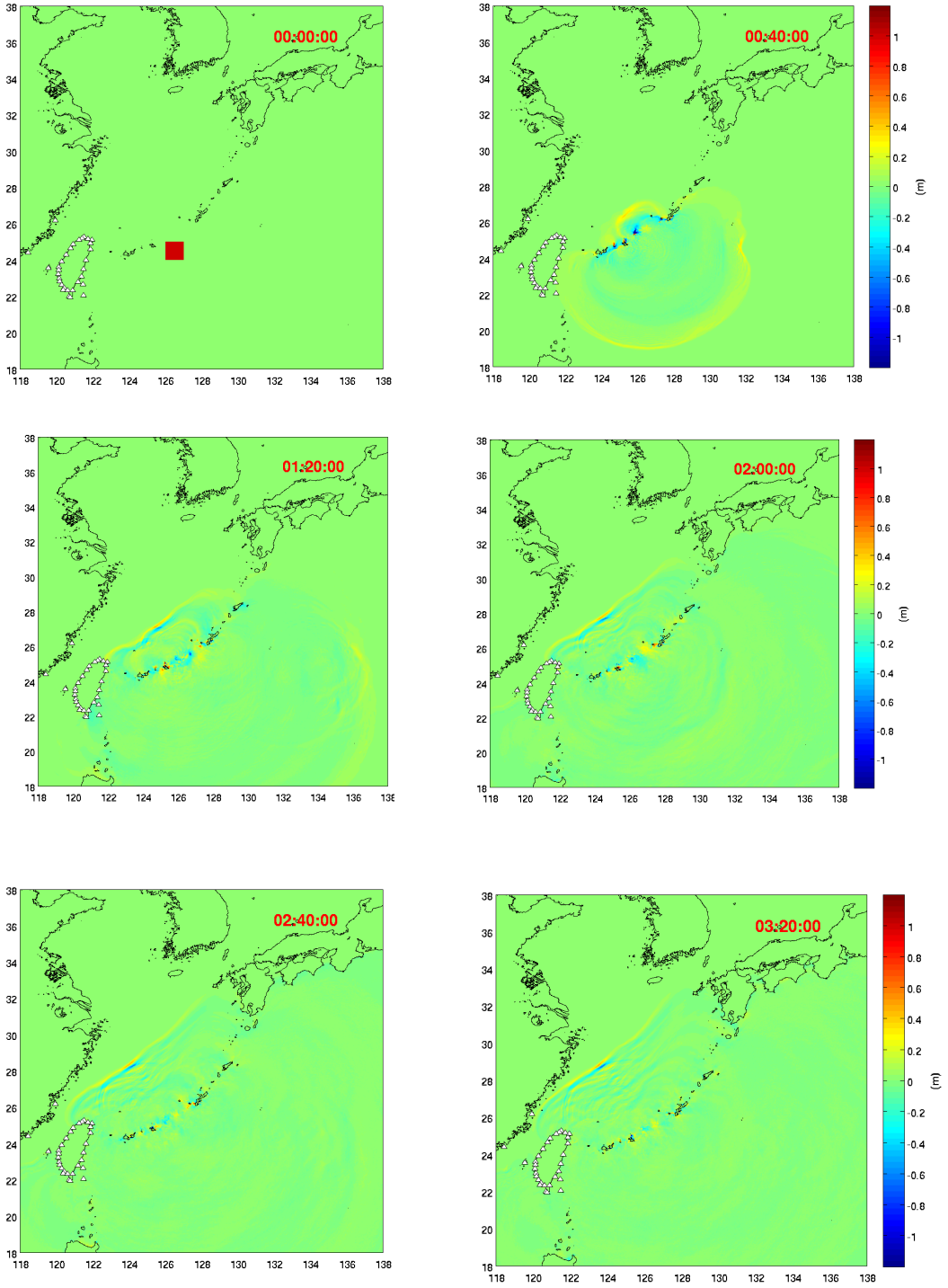

Figure 3: Propagations of an exemplary unit source.

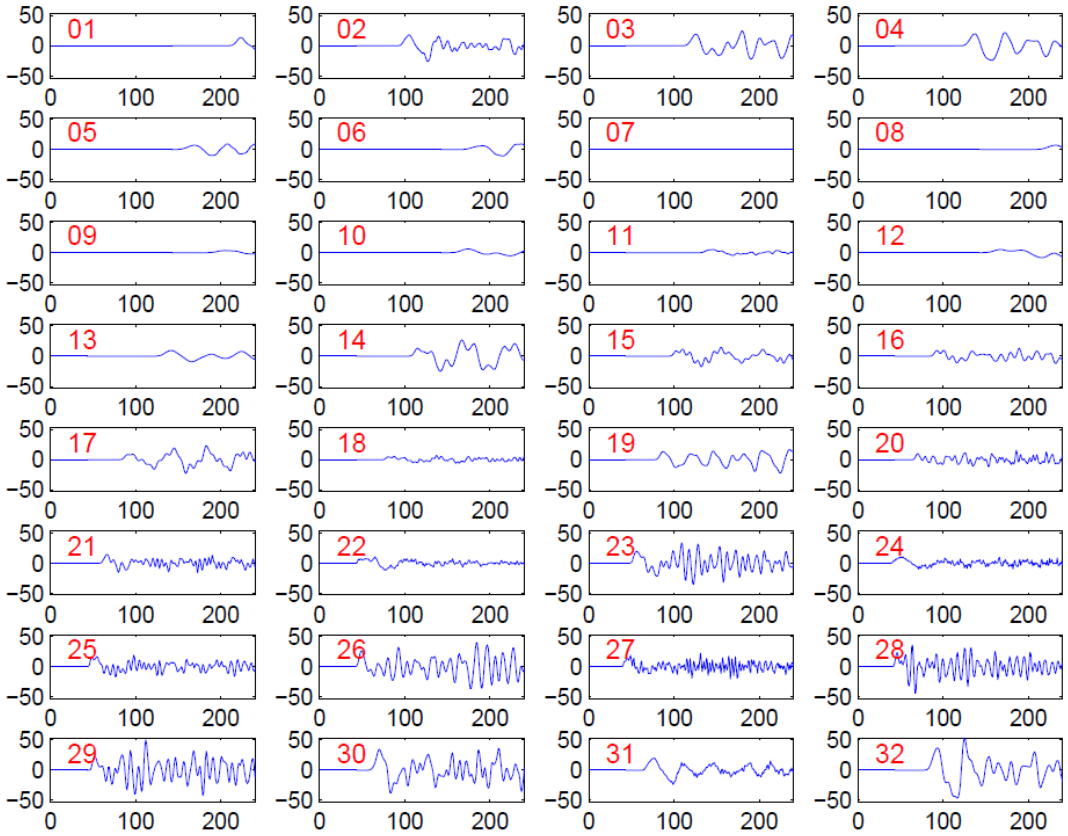

Figure 4: Unit tsunamis of the unit source in Figure 3 for the 32 CWB tidal stations.

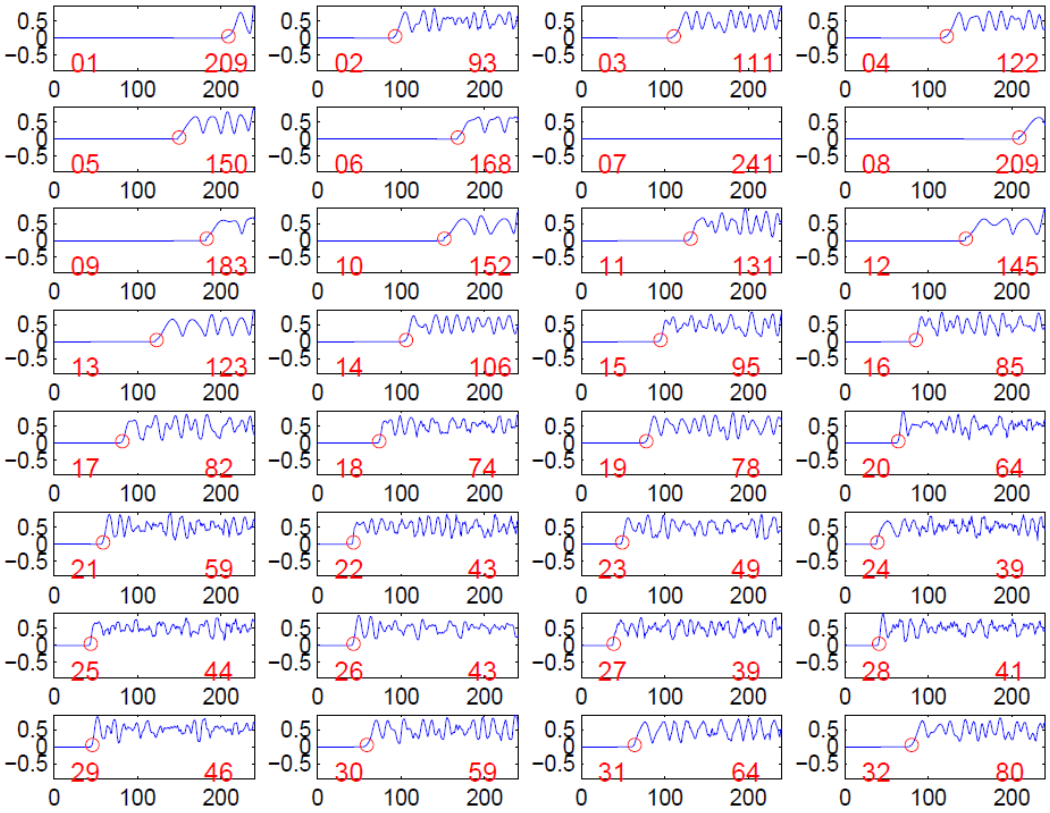

Figure 5: Results of STA/LTA for unit tsunamis in Figure 4. The numbers on the right are the picking arrival times in minutes.

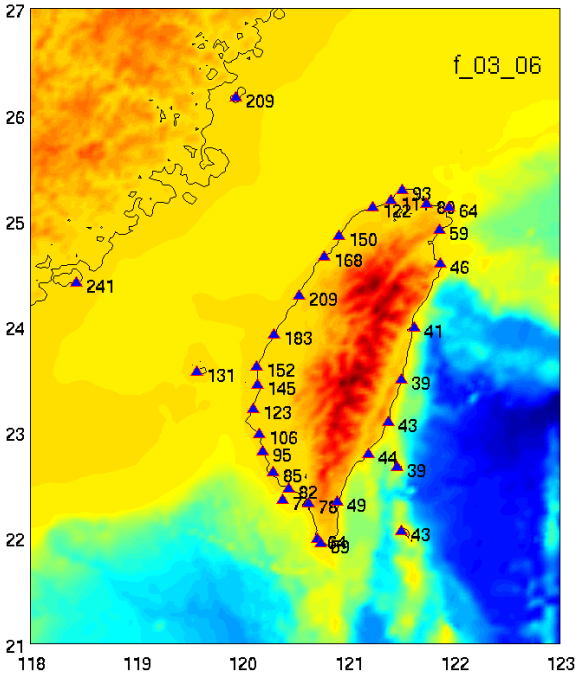

Figure 6: The arrival time map for the unit source in Figure 3.

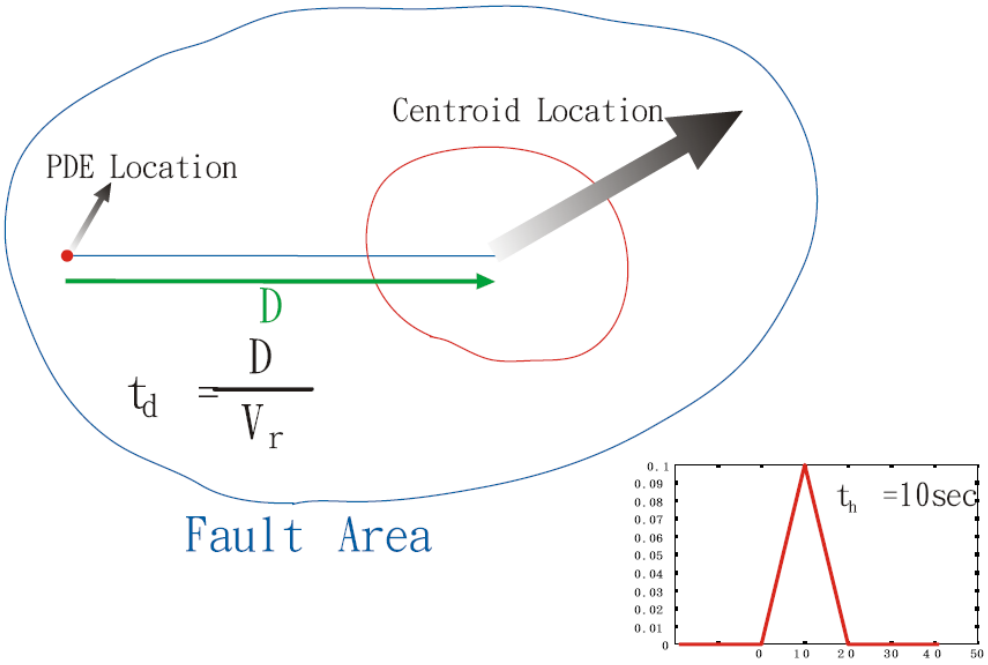

Figure 7: Illustration of the half duration t_h, and centroid delay t_d, schematically. The half duration is the half width of the triangular moment rate function, 10 sec in this example. The centroid delay is the temporal position of the centre of the triangle measured from the assumed origin time, which is the distance (D) between the initial rupture (PDE location) and the centroid location divided by the rupture velocity (V_r).

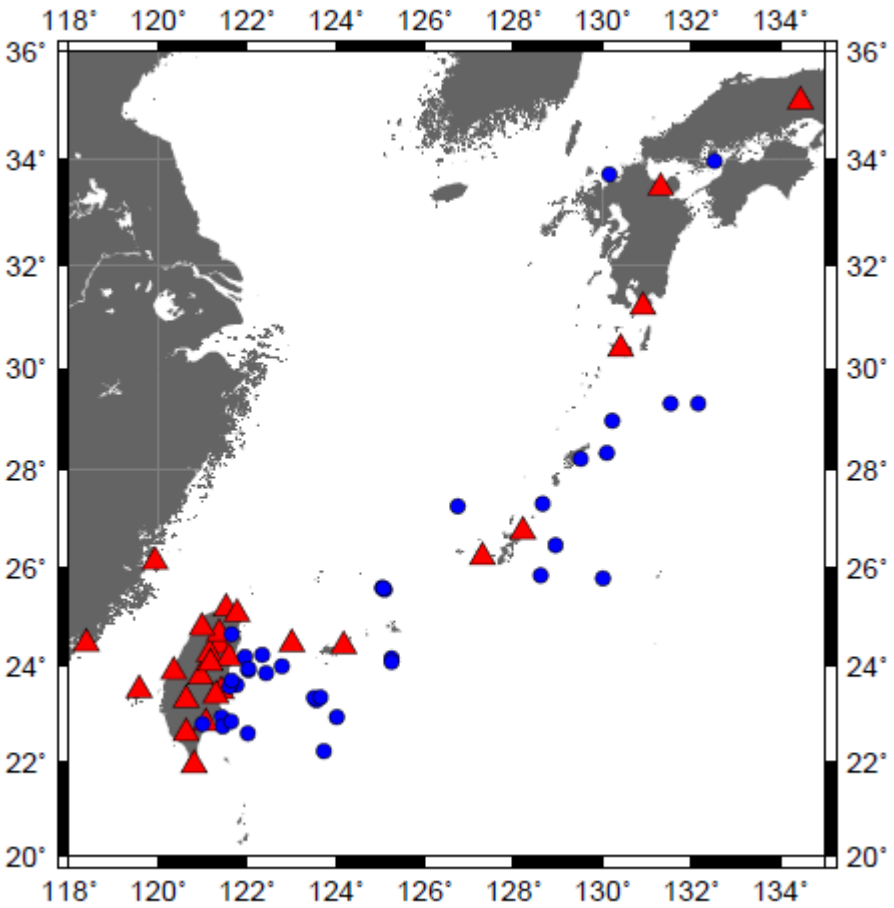

Figure 8: Distributions of earthquakes (circles) associated with the Ryukyu subduction zone for *W* phase inversion. Red triangles are stations where data are collected.

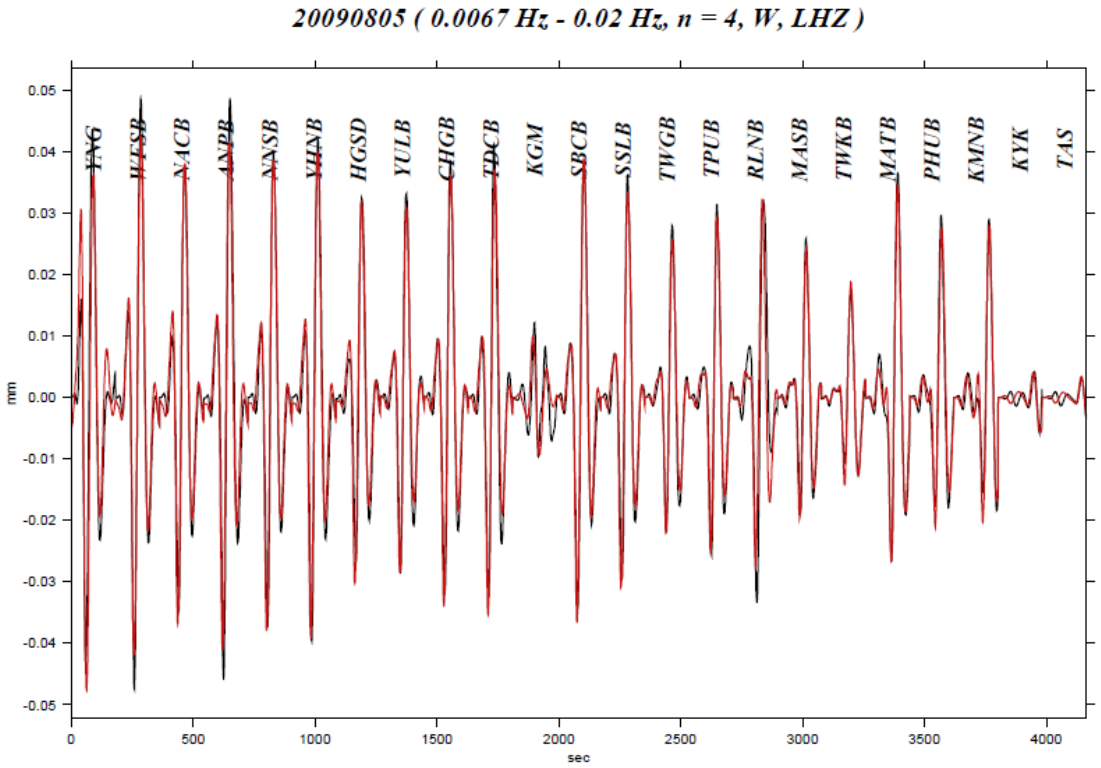

Figure 9: Observed (black) and synthetic (red) *W* phase for the event 20090805. The *W* phase time window of each station is trimmed and concatenated for inversion. Labels are names of stations.

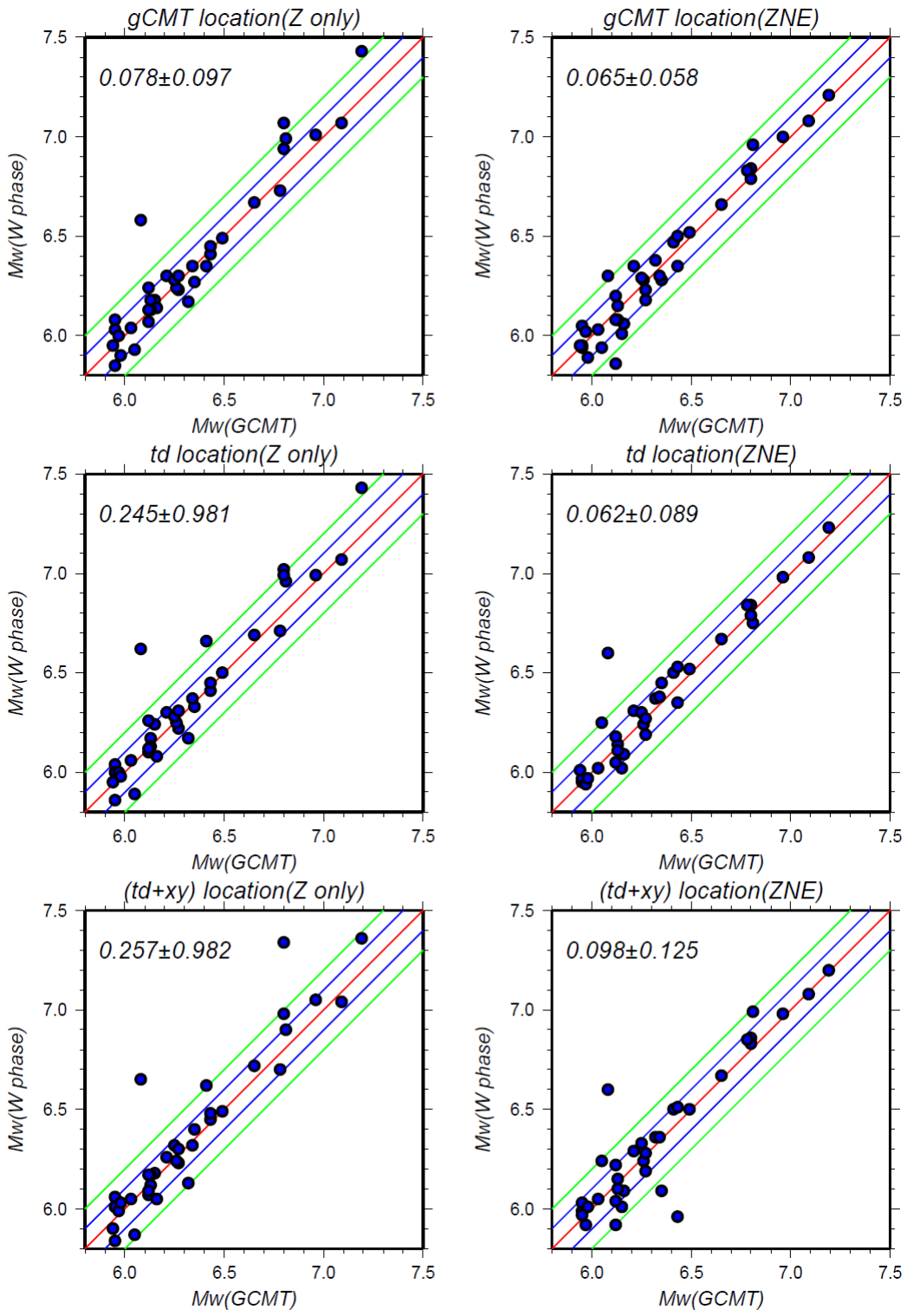

Figure 10: Comparison of M_w (gCMT) and M_w (*W* phase) for earthquakes used in this study. The left column is results of Z component and the right one ZNE components. Top to bottom represents three sets for different level of knowledge on earthquake parameters (see text). Numbers are mean values for differential M_w and standard deviation. The best result is those of gCMT location and the best implementable result is those of t_d location using ZNE components (middle right).